

Accepted Manuscript

Creation of a SIP Lyase Bacterial Surrogate for Structure-Based Drug Design

Maria A. Argiriadi, David Banach, Elzbieta Radziejewska, Susan Marchie, Jennifer DiMauro, Jurgen Dinges, Eric Dominguez, Charles Hutchins, Russell A. Judge, Kara Queeney, Grier Wallace, Christopher M. Harris

PII: S0960-894X(16)30209-8
DOI: <http://dx.doi.org/10.1016/j.bmcl.2016.02.084>
Reference: BMCL 23638

To appear in: *Bioorganic & Medicinal Chemistry Letters*

Received Date: 13 January 2016
Revised Date: 25 February 2016
Accepted Date: 27 February 2016

Please cite this article as: Argiriadi, M.A., Banach, D., Radziejewska, E., Marchie, S., DiMauro, J., Dinges, J., Dominguez, E., Hutchins, C., Judge, R.A., Queeney, K., Wallace, G., Harris, C.M., Creation of a SIP Lyase Bacterial Surrogate for Structure-Based Drug Design, *Bioorganic & Medicinal Chemistry Letters* (2016), doi: <http://dx.doi.org/10.1016/j.bmcl.2016.02.084>

This is a PDF file of an unedited manuscript that has been accepted for publication. As a service to our customers we are providing this early version of the manuscript. The manuscript will undergo copyediting, typesetting, and review of the resulting proof before it is published in its final form. Please note that during the production process errors may be discovered which could affect the content, and all legal disclaimers that apply to the journal pertain.





Creation of a SIP Lyase Bacterial Surrogate for Structure-Based Drug Design

Maria. A. Argiriadi,^{a*} David Banach^b, Elzbieta Radziejewska^b, Susan Marchie^b, Jennifer DiMauro^b, Jurgen Dinges^c, Eric Dominguez^b, Charles Hutchins^c, Russell A. Judge^c, Kara Queeney^b, Grier Wallace^a and Christopher M. Harris^b

* Corresponding author. Tel +1 508 849 2643. E-mail address: maria.argiriadi@abbvie.com

^aAbbVie Bioresearch Center, 381 Plantation Street, Worcester, MA 01605

^bAbbVie Bioresearch Center, 100 Research Drive, Worcester, MA 01605

^cAbbVie, 1 North Waukegan Road, North Chicago, IL 60064

ARTICLE INFO

Article history:

Received

Received in revised form

Accepted

Available online

Keywords:

SIP Lyase

Site-directed mutagenesis

Homology modeling, crystal structure

ABSTRACT

SIP Lyase (SPL) has been described as a drug target in the treatment of autoimmune diseases. It plays an important role in maintaining intracellular levels of SIP thereby affecting T cell egress from lymphoid tissues. Several groups have already published approaches to inhibit SIP Lyase with small molecules, which in turn increase endogenous SIP concentrations resulting in immunosuppression. The use of structural biology has previously aided SPL inhibitor design. Novel construct design is at times necessary to provide a reagent for protein crystallography. Here we present a chimeric bacterial protein scaffold used for protein x-ray structures in the presence of early small molecule inhibitors. Mutations were introduced to the bacterial SPL from *Symbiobacterium thermophilum* which mimic the human enzyme. As a result, two mutant StSPL crystal structures resolved to 2.8 Å and 2.2 Å resolutions were solved and provide initial structural hypotheses for an isoxazole chemical series, whose optimization is discussed in the accompanying paper.

2015 Elsevier Ltd. All rights reserved.

Small molecule drug discovery often requires structural biology to facilitate the design of compounds that can interact with a given target protein. There are instances when protein reagent generation is difficult with hurdles such as low protein yield/solubility or protein conformational heterogeneity. This hampers progression into wide crystallization screening and ultimately iterative crystal structures. Protein construct design can be used to overcome this hurdle. Here we will describe a novel construct approach to provide structural support for the protein target SIP Lyase.

SIP Lyase (SPL) catalyzes the irreversible breakdown of sphingosine-1-phosphate (S1P) into *trans*-2-hexadecenal and ethanolamine phosphate. This activity is critical for maintaining the low S1P tone in secondary lymphoid organs which is essential for normal lymphocyte trafficking.¹ SPL inhibition prevents lymphocyte egress from lymph node, thymus, and spleen, resulting in peripheral lymphopenia and immunosuppression.^{1,2} Therefore this protein has been investigated as a potential target for a range of autoimmune disorders such as rheumatoid arthritis and multiple sclerosis.^{3,4}

SPL is a member of the PLP (pyridoxal 5'-phosphate) superfamily and is located in the endoplasmic reticulum.⁵ Initial SPL structural information of the soluble PLP binding domain

was obtained from both a prokaryotic SPL homolog in *Symbiobacterium thermophilum* (StSPL) and yeast SPL (Dpl1p), which gave the first view of the SPL structural scaffold and key features of the binding pocket.⁶ One of the conclusions from this study was that both prokaryotic and eukaryotic homologs shared the same quaternary fold (overall r.m.s.d 1.2 Å for dimer), with relatively conserved features in the active site and the PLP co-factor binding pocket. Due to our difficulty with protein expression and generation of human SPL for crystallography and based on the strong resemblances between prokaryotic and eukaryotic scaffolds, we embarked on a bacterial surrogate approach to use a more "human-like" mutant version of StSPL to crystallize with our early SPL inhibitor leads. Here we present the surrogate construct strategy and key crystal structures resulting from this effort. The accompanying paper discusses application of these structures for further inhibitor optimization.

Several attempts were made to create human constructs for SPL in order to structurally enable design chemistry efforts. Protein generated from these constructs suffered from poor yields and large aggregation issues. We were fortunate to read the published work of Bourquin and colleagues which presented a high resolution crystal structure of a prokaryotic homolog of SPL from *Symbiobacterium thermophilum* (PDB code 3MAD).⁶

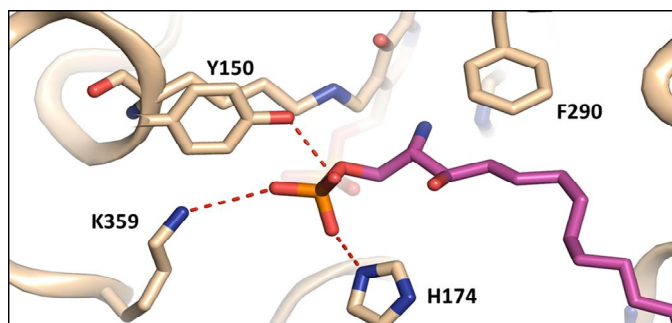


Figure 1a: Model of S1P (magenta) bound to human SPL (tan)

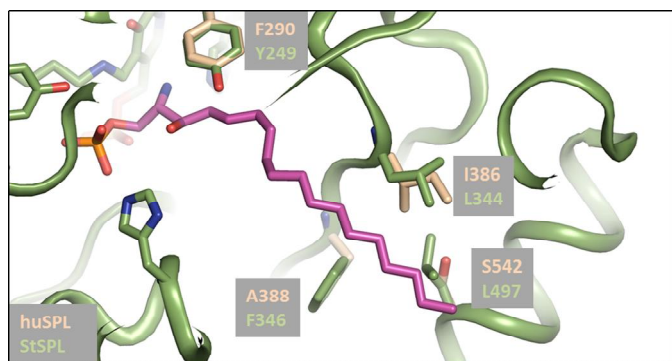


Figure 1b: Overlay of StSPL (green) (PDB code 3MAD⁶) with human SPL (residues shown in tan) which shows four divergent residues proximal to the S1P binding site

Using this crystal structure, a homology model of human (with S1P bound) was generated to observe the potential placement of the natural substrate and the amino acids that surround the substrate.⁷ In the model (shown in Figure 1a), the phosphate of S1P is located in the putative phosphate binding site and makes interactions with residues Y150, K359 and H174. F290 caps the active site forming a fairly narrow channel for the S1P substrate to bind. The active site opening contains an assortment of hydrophobic residues which presumably stabilize the long alkyl tail of the substrate. Based on this modeling hypothesis, we superimposed the high resolution structure of StSPL (PDB code 3MAD) and the human SPL model to observe key residue differences proximal to S1P. While most locations in the active site remained fairly constant (*i.e.*, PLP binding pocket and phosphate binding site), four positions (StSPL: Y249, L344, F346 and L497, Human: F290, I386, A388, S542) showed diversity between the homologs (Figure 1b). Y249 superimposes with the key residue F290 and L344/ L479/L497 line the active site opening to solvent. We then decided to use the StSPL protein scaffold and introduce site-directed mutations at these locations to create a chimeric “human-like” active site for crystallography.

An *E. coli* construct of StSPL 2-570 (Y249F, L344I, F346A, L497S,) was created, which resulted in robust protein expression and final protein yields.⁸ Catalytic activity of this mutant bacterial construct was assessed using a substrate analog in which the C13 hydrocarbon tail of S1P is replaced with an ether-linked umbelliferone group.^{9,10} The K_M of S1P for StSPL is approximately 10-fold lower than human SPL, and its V_{max} is lower by a similar degree (Figure 2). The decrease in V_{max} may simply reflect the added stabilization of the SPL-substrate complex with respect to the reaction transition state, as reflected by the decrease in K_M . At the standard assay condition of 500 μ M substrate, the two constructs have similar specific activities and enable a comparison of IC_{50} values for Compound 1: 0.17 μ M for StSPL and 1.0 μ M for human SPL (not shown). Protein crystals

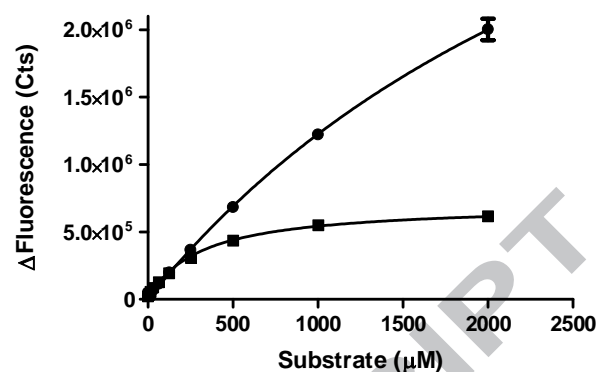


Figure 2: Kinetic characterization of SPL constructs. K_M and V_{max} for mutant StSPL are 310 μ M and 7.1×10^5 cts for mutant StSPL (■) and estimated to be $\geq 2,000$ μ M and 5×10^6 cts for huSPL (●).

in the presence of PLP co-factor were grown and diffracted to high resolution. In parallel, an HTS screen was conducted using the wild-type human enzyme and several compounds were identified as preliminary hits. As an example, Compound 1 (Figure 3) (N-(2-((4-methoxy-2,5-dimethylbenzyl)amino)-1-phenylethyl)-5-methylisoxazole-3-carboxamide) was identified with modest potency with an IC_{50} of 1.0 μ M. This compound was used in crystal-soaking procedures in hopes of obtaining a ligand bound StSPL mutant crystal structure. At that time, we needed structural guidance to provide a binding mode, preferred chirality, and design opportunities for optimization of this isoxazole-amide chemotype.

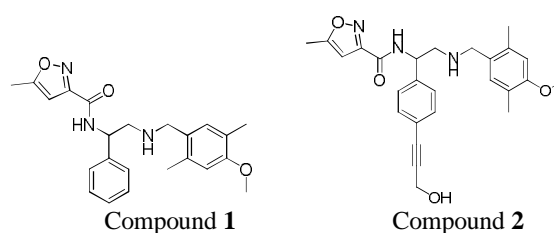


Figure 3: **Compound 1** N-(2-((4-methoxy-2,5-dimethylbenzyl)amino)-1-phenylethyl)-5-methylisoxazole-3-carboxamide **Compound 2** N-(1-(4-(3-hydroxyprop-1-yn-1-yl)phenyl)-2-((4-methoxy-2,5-dimethylbenzyl)amino)ethyl)-5-methylisoxazole-3-carboxamide

A 2.8 Å resolution structure of Compound 1 bound to the StSPL mutant was solved with reasonable refinement statistics (Figure 4).¹¹ The overall structure had high similarity to the previously reported (PDB code 3MAD) structure with an overall r.m.s.d of 0.4 Å.⁶ Additionally, when comparing this crystal structure to the recently reported human SPL structure (PDB code 4Q6R⁴), we noticed a strong similarity to backbone and side chain placement in the active site. Electron density was observed in both active sites and both Compound 1 and PLP could be modeled in the density. The binding mode of Compound 1 assumes a “wishbone” conformation due to the flexible nature of the molecule and reaches to several regions in the SPL active site proximal to the PLP cofactor (Figure 4). The 3D structure confirms an S-isomer stereochemistry where the ligand is stabilized by several contacts with the protein. For example, there is a clear edge-to-face interaction of Compound 1’s central phenyl ring with nearby StSPL residue Y345. Beyond the central phenyl is a crystallographic water which lies close to the bound phosphate and PLP cofactor. The ligand wishbone conformation

is further stabilized by two hydrogen bonds: the amine N bound to the backbone carbonyl of I344 and the amide carbonyl to the backbone N of A346. The isoxazole binds in a shallow channel outlined by residues from both monomers: F500/L504 (monomer A) and P348 (monomer B). The methoxy benzyl projects towards the active site entrance and is surrounded by aromatic residues Y481 and F500. The N-terminus of the protein was disordered and as previously hypothesized might serve as a flexible gate which closes the ligand-bound active site from solvent.⁶

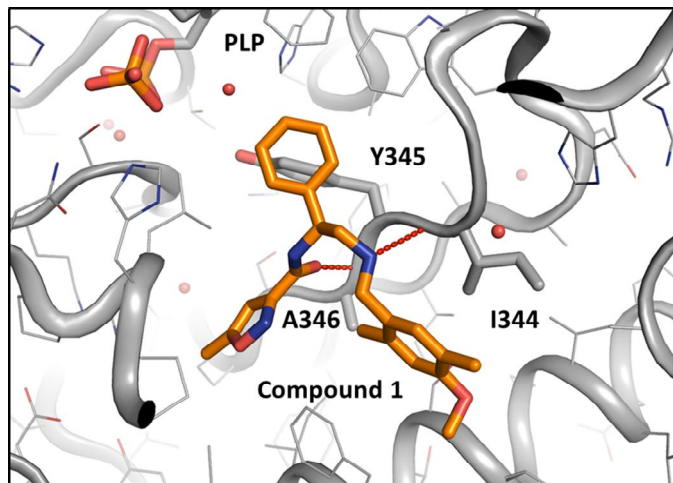


Figure 4: Crystal structure of StSPL mutant (grey) bound to Compound 1

This initial structure of Compound 1 bound to the surrogate SPL drove medicinal chemistry design strategies to improve its inhibition. Several ideas emerged: 1) rigidification of the wishbone linkages to remove rotational freedom 2) optimization of both the isoxazole and benzyl methoxy rings to improve induced fit in their respective binding pockets, and 3) *para* substitution off of the central phenyl ring to interact or replace the crystallographic water near the PLP co-factor. Here, we will focus on the third strategy.

As mentioned previously, the central phenyl ring is positioned near a crystallographic water with ample pocket volume for potential substitution. Superimposing the models of SIP and Compound 1 suggests a substitution at the *para* position of the phenyl ring in Compound 1 to either replace or interact with the water. Several attempts were made to design into this region resulting in Compound 2 (Figure 3) which introduces an alkyne linking segment capped with an -OH to replace the crystallographic water. This substitution proved to be successful in moderately improving the IC₅₀ to 0.15 μ M. When solving the structure of Compound 2 bound to StSPL, we were fortunate to collect higher resolution data with the opportunity to model more water molecules.¹¹ Compound 2 binds identically to Compound 1 with the alkyne-hydroxyl capping group replacing the water identified in the first crystal structure (Figure 5). Interestingly, the hydroxyl taps into a larger solvent network which engages the the PLP co-factor. Specifically, the group hydrogen bonds to a nearby water which in turn binds to the phosphate of PLP and nearby residue Y345. Therefore Compound 2 fills productive VDW space with its alkyne linkage and improves the active site solvent network with its hydroxyl. We were happy to see that the mutant StSPL surrogate crystal structures provided us with a successful hypothesis regarding the 3D solvent environment. This in turn helped identify a key potency driver in the SPL active site. After our structural work was completed, the human structure of SPL (PDB code 4Q6R)⁴ was published which provided additional retrospective support to our strategy. An

identical solvent network was observed in the human structure at this location with a succinic acid molecule in the place of Compound 2's alkyne alcohol (Figure 6). It was intriguing that initial structural observations seen in the bacterial structural surrogate were similar to those in the human SPL crystal structure.

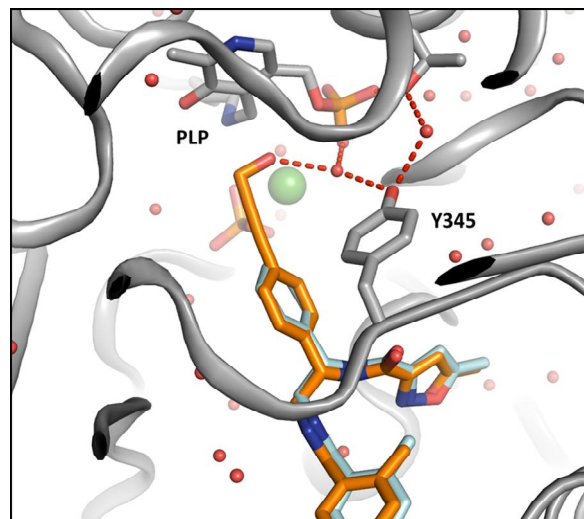


Figure 5: Crystal structure of mutant StSPL and Compound 2 (orange) gives structural rationale for improved potency *via* solvent network. Compound 2 is overlaid with Compound 1 (light blue) to show comparable binding modes. The green sphere illustrates the water identified in the StSPL/Compound 1 structure and replaced in the StSPL/Compound 2 structure.

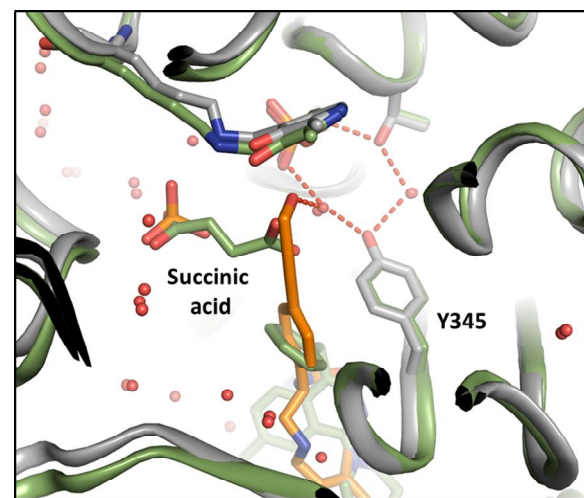


Figure 6: Solvent network in mutant StSPL complexed to Compound 2 as it compares to human SPL (PDB code 4Q6R).⁴

Here we present a surrogate crystallographic approach for the target protein SIP Lyase. In the absence of well-behaved human protein, we chose a surrogate crystallographic approach to guide initial medicinal chemistry design. A construct was designed to incorporate mutations which mimicked the human active site. Protein generated from this construct was tested for activity and used for crystallography. As a result, two key crystal structures were solved and provided some initial structural hypotheses which aided the design of subsequent analogs, which is discussed in the accompanying paper. These compounds and analogs showed efficacious activity against human SPL providing a lead chemical series.

Acknowledgments

All authors are employees of AbbVie. The design, study conduct, and financial support for this research were provided by AbbVie. AbbVie participated in the interpretation of data, review, and approval of the publication.

The HTS hit Compound **1** was identified by Hetal Patel.

All structural figures were created in the program Pymol.¹³

Use of the IMCA-CAT beamline 17-ID (or 17-BM) at the Advanced Photon Source was supported by the companies of the Industrial Macromolecular Crystallography Association through a contract with Hauptman-Woodward Medical Research Institute. Use of the Advanced Photon Source was supported by the U.S. Department of Energy, Office of Science, Office of Basic Energy Sciences, under Contract No. DE-AC02-06CH11357.

Supplementary data

Supplementary data (crystallographic data and additional experimental procedures) associated with this article can be found, in the online version, at doi:

References and notes

- Schwab, S. R.; Pereira, J. P.; Matloubian, M.; Xu, Y.; Huang, Y.; Cyster, J. G. *Science* **2005**, *309*, 1735.
- Vogel, P.; Donoviel, M. S.; Read, R.; Hansen, G. M.; Hazlewood, J.; Anderson, S. J.; Sun, W.; Swaffield, J.; Oravecz, T.; *PLoS One* **2009**, *4*(1):e4112.
- Bagdanoff, J. T.; Donoviel, M. S.; Nouralddeen, A.; Tarver, J.; Fu, Q.; Carlsen, M.; Jessop, T. C.; Zhang, H.; Hazlewood, J.; Nguyen, H.; Baugh, S. D.; Gardyan, M.; Terranova, K. M.; Barbosa, J.; Yan, J.; Bednarz, M.; Layek, S.; Courtney, L. F.; Taylor, J.; Digeorge-Foushee, A. M.; Gopinathan, S.; Bruce, D.; Smith, T.; Moran, L.; O'Neill, E.; Kramer, J.; Lai, Z.; Kimball, S. D.; Liu, Q.; Sun, W.; Yu, S.; Swaffield, J.; Wilson, A.; Main, A.; Carson, K. G.; Oravecz, T.; Augeri, D. J. *J. Med. Chem.* **2009**, *52*, 3941.
- Weiler, S.; Braendlin, N.; Beerli, C.; Bergsdorf, C.; Schubart, A.; Srinivas, H.; Oberhauser, B.; Billich, A. *J. Med. Chem.* **2014**, *57*, 5074.
- Van Veldhoven, P. P.; Mannaerts, G.P. *Adv. Lipid. Res.* **1993**, *26*, 69.
- Bourquin, F.; Riezman, H.; Capitani, G.; Grutter, M. G. *Structure* **2010**, *18*, 1054.
- A human SPL homology model was created using the program InsightII (InsightII, Accelrys Inc., San Diego, USA, **1998**) and using the known crystal structure of 3MAD *Symbiobacterium thermophilum* SPL (NCBI YP_075103) as a template.⁶ Comparison of the human model and the bacterial crystal structure showed 4 amino acid positions that were different in the active site proximal to the location of the PLP binding site. These positions were mutated in the bacterial S1P Lyase to create a "human-like" SPL active site using the overall bacterial protein scaffold. Quadruple mutations Y249F, L344I, F346A, L497S were introduced to the sequence (2-507) using a pQE70 vector, T5 promoter.
- Recombinant pQE70 Symbio SPL 2-507 (Y249F, L344I, F346A, L497S)-His6 was produced from a high density expression using XL1 Blue competent cells after 20 hours of growth induced culture for 4 hr at 30°C with 2% ethanol and 0.1 mM IPTG. Cell paste was stored at Quu -80°C and subsequently thawed to 4°C. Lysis buffer contained 50 mM Phosphate pH 7.2, 2 mM BME, 0.4 mM pyridoxal phosphate (PLP), benzoase and protease inhibitors. Soluble extract was collected after centrifugation (GSA rotor, 17,000 rpm, 25 min). The supernatant was applied to a Nickel affinity column (GE Healthcare Life Sciences) and mutant StSPL protein was eluted with 50 mM Phosphate, pH 7.2, 2 mM BME, 0.4 mM pyridoxal (Buffer A) + 10 mM imidazole. The pooled sample (mutant StSPL + PLP complex) was concentrated and loaded onto a Superdex 200 column (GE Healthcare, Life Sciences) with Buffer B: 50 mM Phosphate pH 7.2, 100 mM NaCl, 1 mM EDTA, 1 mM DTT and 0.01 mM PLP. Two major mutant StSPL peaks eluted corresponding to monomer and dimeric peaks of StSPL. Dimer-pooled samples were concentrated to 11 mg/ml and used for crystallography and assay work. Sample purity was assessed with SDS-PAGE
- Bedia, C.; Camacho, L.; Casas, J.; Abad, J. L.; Delgado, A.; Van Veldhoven, P. P.; Fabriàs, G. *Chem. Bio. Chem.* **2009**, *10*, 820.
- Enzyme activity assays were performed by a variation of the method developed by Bedia and colleagues.⁹ The following components were added to 96 half-well plates: 20 µL compound solution in 10% DMSO/90% water, 10 µL 2 mM substrate, and 10 µL 50 nM S1P Lyase with 50 µM pyridoxal-5'-phosphate. Human S1P Lyase was purchased from BPS Biosciences. Substrate and enzyme were formulated in 200 mM potassium phosphate, pH 8.0, 0.6 mM EDTA, 0.3 M NaCl, 20% glycerol, 50 mM NaF, and 0.1% Tween-20. Reactions were incubated at room temperature for 22 hr, following which umbelliferone fluorescence was read with excitation at 380 nm and emission at 460 nm. IC₅₀ values were analyzed by least-means-squares fitting to the following equation: Percent Activity = 100/(1+([inhibitor]/IC₅₀)). Assay precision was determined from a set of 30 compounds with repeat data by calculation of a Test/Re-test Mean Significant Ratio of 2.3, according to published methods.¹²
- Atomic coordinates and structure factors have been deposited to the Protein Data Bank (www.rcsb.org). PDB codes are 5EUE and 5EUD.
- Beck, G.; Chen, Y.-F.; Dere, W.; Devanarayan, V.; Eastwood, B.J.; Farmen, M.W.; Iturria, S.J.; Iversen, P.W.; Kahl, S.D.; Moore, R.A.; Sawyer, B.D.; Weidner, J. Assay Operations for SAR Support. 2012 May 1 [Updated 2012 Oct 1]. Sittampalam, G.S.; Coussens, N.P.; Nelson, H.; Arkin, M.; Auld, D.; Austin, C.; Bejcek, B.; Glicksman, M.; Inglese, J.; Iversen, P.W.; Li, Z.; McGee, J.; McManus, O.; Minor, L.; Napper, A.; Peltier, J.M.; Riss, T.; Trask, O.J. Jr.; Weidner, J., editors. Assay Guidance Manual [Internet]. Bethesda (MD): Eli Lilly & Company and the National Center for Advancing Translational Sciences; 2004-. Available from: <http://www.ncbi.nlm.nih.gov/books/NBK91994/>
- The PyMOL Molecular Graphics System, Version 1.2r3pre, Schrödinger, LLC

Graphical Abstract

To create your abstract, type over the instructions in the template box below.

Leave this area blank for abstract info.

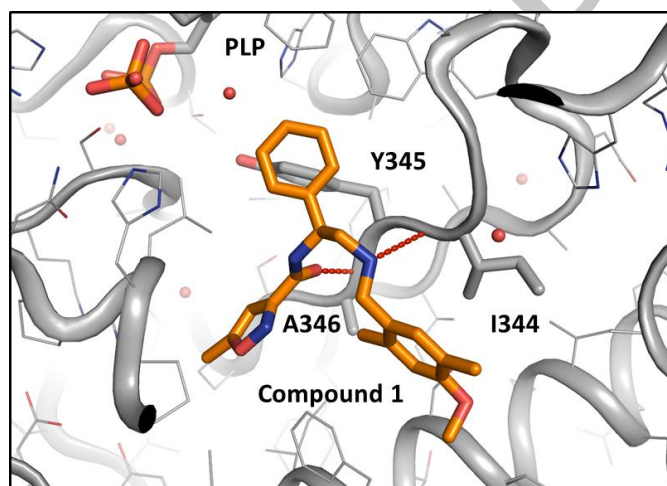
Creation of a S1P Lyase Bacterial Surrogate for Structure-Based Drug Design

Maria. A. Argiriadi,^{a*} David Banach^b, Elzbieta Radziejewska^b, Susan Marchie^b, Jennifer DiMauro^b, Jurgen Dinges^c, Eric Dominguez^b, Charles Hutchins^c, Russell A. Judge^c, Kara Queeney^b, Grier Wallace^c and Christopher M. Harris^b

^aAbbVie Bioresearch Center, 381 Plantation Street, Worcester, MA 01605

^bAbbVie Bioresearch Center, 100 Research Drive, Worcester, MA 01605

^cAbbVie, 1 North Waukegan Road, North Chicago, IL 60064



Fonts or abstract dimensions should not be changed or altered.